Sexually dimorphic traits and male-specific differentiation are actively regulated by Doublesex during specific developmental windows in *Nasonia vitripennis*

Yidong Wang [a], Anna Rensink [b], Ute Fricke [a,*], Megan C. Riddle [c,$], Carol Trent [c], Louis van de Zande [b], Eveline C. Verhulst [a,d]

a. Wageningen University, Laboratory of Entomology, Wageningen, The Netherlands
b. Evolutionary Genetics, Development and Behaviour, Groningen Institute for Evolutionary Life Sciences, University of Groningen, Groningen, The Netherlands
c. Biology Department, Western Washington University, Washington, United States of America
d. Wageningen University, Laboratory of Genetics, Wageningen, The Netherlands

* Current address: Departement of Animal Ecology and Tropical Biology, Biocenter, University of Würzburg, Würzburg, Germany

$ Current addresses: Department of Psychiatry and Behavioral Sciences, University of Washington, Seattle, WA, United States of America; Eating Recovery Center
1231 116th Ave NE Suite 800, Bellevue, WA 98004

Corresponding author: eveline.verhulst@wur.nl

Keywords: *Nasonia,* Doublesex, sexually dimorphic traits, sexual differentiation, parasitoid wasps, sex determination

Abstract

Sexually dimorphic traits in insects are rapidly evolving due to sexual selection which can ultimately lead to speciation. However, our knowledge of the underlying sex-specific molecular mechanisms is still scarce. Here we show that the highly conserved gene, *Doublesex (Dsx),* regulates rapidly diverging sexually dimorphic traits and differentiation in the model parasitoid wasp *Nasonia vitripennis* (Hymenoptera: Pteromalidae). We present here the revised full *Dsx* gene structure with an alternative exon one and two additional male *NvDsx* isoforms, which gives important insights into the evolution of the sex-specific oligomerization domains and C-termini. We show the sex-specific *NvDsx* expression throughout development, and demonstrate that transient *NvDsx* silencing in different male developmental stages dramatically shifts the morphology of two sexually dimorphic traits from male to female, with the effect being dependent on the timing of silencing. In addition, transient silencing of *NvDsx* in early male larvae affects male genitalia tissue growth but not morphology. This shows that male *NvDsx* is actively required to suppress female-specific traits and promote male-specific traits during specific developmental windows. These results also strongly suggests that in *N. vitripennis* most sex-specific tissues fully differentiate in the embryonic stage and only need *NvDsx* input for growth afterwards. This provides a first insight into the regulatory activity of *Dsx* in Hymenoptera and will help us to better understand the evolutionary and molecular mechanisms involved in sex-specific development, which can eventually lead to the development of new synthetic genetics-based tools for biological pest control by parasitoid wasps.

Significance Statement

In insects, male and female differentiation is regulated by the highly conserved transcription factor *Doublesex* (*Dsx*). The role of *Dsx* in regulating rapidly evolving sexually dimorphic traits has received less attention, especially in wasps and bees. Here, we mainly focused on *Dsx* regulation of two sexually dimorphic traits and male genitalia morphology in the parasitoid wasp, *Nasonia vitripennis.* We demonstrate that *Dsx* actively regulates male-specific tissue growth and morphology during specific developmental windows. These findings will help us to better understand the molecular mechanisms underlying the rapid evolution of sexual differentiation and sexually dimorphic traits in insects, but may also be the starting point for the development of new tools for biological control of pest insects by parasitoid wasps.

Introduction

Insects are well known for their distinct differences between male and female morphology.

The reproductive organs and sexually dimorphic traits such as wing shapes and colour patterns are one of the fastest evolving traits in insects and are therefore often used to distinguish species, as these traits can differ dramatically between species. Development of these fast changing sexually dimorphic traits usually depends on specific genes that are expressed tissue and sex specifically (1). Many of these genes are under control of the transcription factor, Doublesex (Dsx), that initiates sexual differentiation in insects (2–4). *Dsx* pre-mRNA is alternatively spliced to yield male-specific *Dsx* (*DsxM*) or female-specific *Dsx* (*DsxF*) transcripts, resulting in distinct sex-specific protein isoforms (5). Two functional domains are present in all insect Dsx homologs: 1) the DM domain which consists of a DNA binding domain (DBD) and an oligomerization domain (OD1) with a zinc module and binding sites to facilitate binding downstream targets; 2) a dimerization domain (OD2) with a common N-terminal part and a sex specific C-terminal part. These C-terminal sex-specific differences are assumed to be involved in the regulation of the development of sex-specific traits (6,7). For instance, in *Drosophila,* DsxM represses and DsxF activates the expression of *bric-à-brac (bab)* which results in male-specific abdominal pigmentation (8). A similar action is observed in the formation of sex combs, an important feature for performing mating rituals in males of some *Drosophila* species (9). In *Bactrocera dorsalis, DsxF* knockdown in females triggers the interruption of yolk protein gene expression, leading to ovipositor deformation and a delay in ovary development which confirms the essential role of DsxF to initiate and maintain female development in Diptera (10). In Lepidoptera (butterflies and moths) and Coleoptera (beetles), sex-specific *Dsx* expression in both sexes also affects many sex specific traits. For example, transient expression of *DsxM* in female silkmoths *Bombyx mori* distorts the development of female-specific genital organs by partially introducing male characters in female genitalia (11), and introducing mutations in the male-specific *Dsx* isoform of *B. mori* yields either malfunctioning males or intersexes (12). In *Papilio polytes* butterflies differential expression of *Dsx* isoforms results in sex-specific wing patterns (13). *Dsx* also either promotes or constrains the mandible growth in males and females of *Cyclommatus metallifer* beetles (14), and the formation of head horns in *Trypoxylus dichotomus* beetles is antagonistically regulated by *DsxM* and *DsxF*, while the thoracic horn formation is *DsxM* independent (15,16). Noteworthy, all these experiments were conducted only in a specific developmental stage and only few focused on sexually dimorphic traits. However, the expression of *Dsx* starts in early embryogenesis and continues through maturity which implies its ongoing action (10,17,18).

Thus far, the specific role of *Dsx* in regulating sexually dimorphic traits has not been studied in the Hymenoptera. *Dsx* sex-specific splice variants and expression differences have been identified in honeybees, (*Apis mellifera*), bumble bees (*Bombus ignites),* Japanese ants

72 (*Vollenhovia emeryi*) and fire ants (*Solenopsis invicta*) (19–23), but the role of *Dsx* in
73 regulating reproductive organ development in males has only been shown in sawflies, *Athalia*
74 *rosae* (24). However, to understand the rapid evolution of sexual dimorphism in other insect
75 orders and to compare the molecular mechanisms of *Dsx*-mediated regulation, it is
76 paramount to gain more knowledge on how *Dsx* directs sex-specific and sexually dimorphic
77 trait development in Hymenoptera. Therefore, we set out to 1) identify the sex-specific traits
78 that are regulated by *Dsx* and 2) study the timing by which *Dsx* regulates these traits during
79 development in the parasitoid wasp *Nasonia vitripennis*.

80 *N. vitripennis* belongs to the genus *Nasonia* (*Hymenoptera: Pteromalidae*), and has become
81 the model system for parasitoids as it is highly suitable for evolutionary and developmental
82 genetic studies. Multiple sexually dimorphic traits within the genus *Nasonia* makes it a perfect
83 system to study sex differentiation (25,26). For instance, the femur of hind legs and antennae
84 of female *Nasonia* are pigmented and have a dark-brown color, whereas in males these are
85 pale yellow (26). Only in *N. vitripennis,* males have dramatically shorter forewings and are
86 flightless, (26), while the females can fly and have large forewings in all species. Although
87 *Dsx* has been identified in *N. vitripennis* (27), its role in regulating these sexually dimorphic
88 traits has not been shown before. Previous research identified one male *Dsx* (*NvDsxM*) and
89 one female *Dsx* (*NvDsxF*) splice variant (27) and showed that the conserved splicing factor
90 transformer (Nvtra) is responsible for female-specific splicing of *Dsx* transcripts, while the
91 male-specific *Dsx* transcript is spliced by default into the male isoform (28).

92 To assess the role of *Dsx* in regulating sexual dimorphy in *Nasonia,* we first revisited the
93 *NvDsx* genetic structure. We confirmed existing splice-variants and identified an alternative
94 starting exon and two additional male *NvDsx* splice-variants. We then used RNA interference
95 to temporally silence *Dsx* in different male developmental stages to study its function in
96 sexual differentiation and dimorphism. We found that transient silencing of *NvDsx* in males
97 leads to the emergence of different female-specific morphological traits with the effect being
98 dependent on the timing of silencing during development. In addition, transient silencing of
99 *NvDsx* in early male larvae affects male genitalia tissue growth but not morphology. This
100 indicates that the appearance of these sexually dimorphic traits depends on the action of
101 *NvDsx* in a very specific time window during development. Sex-specific tissue differentiation
102 appears to occur only during embryonic development and constitutive *NvDsx* expression is
103 required to further promote the growth of the reproductive systems, which has not been
104 reported in other insect systems (24,29). Ultimately, our results provide a great start to study
105 the molecular basis of sexual differentiation and rapidly evolving sexual dimorphism in insects

106 in general and particularly in Hymenoptera.

107 **Results and discussion**

108 **Identification and characterization of two additional male-specific *Dsx* splice variants**

109 Previously, only one female (*NvDsxF*) and one male (*NvDsxM*) *Dsx* splice form were
110 identified in *Nasonia vitripennis* (27). The *NvDsxF* splice variant shared the same first 4 exons
111 with the *NvDsxM* splice variant, but 108 bases are spliced out from exon 5 which leads to
112 female-specific exons 5F and 6F. In *NvDsxM* exon 5M results from retaining this 108bp
113 intron which has not been observed in other insects (27) (Fig. 1, *NvDsxF* and *NvDsxM1*). This
114 splice isoform translates into a Dsx protein with a very short OD2 domain of only four amino
115 acids. This *NvDsx* gene structure does not resemble any previously published *Dsx* structures.
116 To investigate the possibility of additional splice variants of *Dsx* pre-mRNA in *N. vitripennis*
117 we performed extensive 5' and 3' RACEs. The results revealed a novel alternative starting
118 exon that we designated exon 1' (Fig. 1). Note that the start codon of protein translation is in
119 exon 2. Using RT-PCR to target exon 1' to exon 5 we verified its presence in transcripts of
120 both sexes but with a higher frequency in female transcripts (Fig. S1). Alternative splicing at
121 the 5' end has not been shown for *Dsx* before. We assume the alternative exon is used in all
122 splice variants (Fig. 1) but long-read RNA sequencing would be required to confirm this. From
123 here on we refer to the alternative variants collectively. The 3' RACEs identified two additional
124 longer male splice variants (Fig. 1). We designated the previously published male-specific
125 variant *NvDsxM1* (MT043363); the newly found longer male splice forms were designated
126 *NvDsxM2* (M2: MT043359; M2': MT043360) and *NvDsxM3* (M3: MT043361; M3': MT043362).
127 All male isoforms share exons 1 (or 1') to 5 with the female isoform *NvDsxF* (MT043364). The
128 *NvDsxM2* open reading frame ends with a stop codon in exon 8 and translates into a protein
129 of 328 amino acids (aa) which is 105 aa longer than the open reading frame of *NvDsxM1*.
130 Compared to *NvDsxM2* we find that exon 8 is skipped in *NvDsxM3* which puts the stop codon
131 in exon 9 yielding a protein of 330 amino acids. These additional male specific splice variants
132 skip the female-specific exon 6 completely which is a shared feature of male splice forms in
133 many different insect species including fruit flies (*D. melanogaster*) (30) (Fig. 1), wild
134 silkmoths (*Antheraea assama*) (31), honeybees (*A. mellifera*) (21) and ants (*S. invicta*) (20).
135 We did not find any non-sex specific splice variants in *N. vitripennis* as opposed to *A.*
136 *mellifera* (Fig. 1) (21). NvDsxM2 and NvDsxM3 protein isoforms are completely identical and
137 only differ at the C-terminus after the male-specific OD2 domain, while NvDsxM1 has a male-
138 specific OD2 domain of only 4 aa (Fig. S6A).

139 ***NvDsxM2* and *NvDsxM3* are spliced by default**

140 To determine whether the additionally identified splice variants are not exclusively expressed
141 in females, we first observed the overall expression of different *Nvdsx* splice forms in both
142 males and females. Across development, *NvDsxF* is only expressed in females while
143 *NvDsxM1, NvDsxM2* and *NvDsxM3* are highly expressed in males (Fig. S2), and expressed
144 at a low level in females. Interestingly, only in males a slight increase of *NvDsxM1, -2 and -3*
145 expression from 36h toward the early pupal stage was observed. Afterwards, the expression
146 remained relatively constant until adult stage (Fig. S2). Overall, *NvDsxM2* is more abundant
147 than *NvDsxM3* (Fig. S2). Females express *NvDsxM1*, *NvDsxM2* and *NvDsxM3* at a low level
148 probably due to the leaky default splicing of male-specific transcripts (Fig. 2B and Fig. S2).
149 Additionally, we studied the effect of *Nvtra* silencing on *Nvdsx* splicing in females as male-
150 specific splice variants are processed by default and do not depend on NvtraF regulation.
151 This means that all three male splice variants should be higher expressed in females after
152 *Nvtra* silencing as there is less NvtraF to regulate splicing of all *Nvdsx* transcripts into the
153 female-specific form. We have shown previously that *Nvtra* pRNAi knockdown in the female
154 pupal stage leads to a shift in splicing from *NvtraF* to *NvtraM* (28). This indeed induced a shift
155 from *NvDsxF* to *NvDsxM* (now *NvDsxM1*) splicing in both the treated adult females and the
156 offspring, without consequences for adult female fertility (28). To verify the default and NvTra
157 independent splicing of *NvDsxM2* and *NvDsxM3*, we used *Nvtra* RNA interference in the last
158 larval instar (4th instar) of females followed by RT-PCR amplification of the different *NvDsx*
159 and *Nvtra* splice variants from 3 hours post injection (hpi) to 5 days post injection (dpi). After
160 confirming that *Nvtra* RNAi leads to *NvtraM* splicing in females (Fig. 2), we did not observe a
161 clear reduction of female *NvDsxF* expression. Instead, a minor increase of *NvDsxM1*
162 expression from 4dpi onwards was observed. *NvDsxM2* and *NvDsxM3* expression levels did
163 increase substantially from 1dpi onward compared to *gfp* knockdown control.

164 **NvDsxM represses female-specific pigmentation**

165 To assess the sex-specific function of Dsx, we studied the phenotypic effect of *NvDsx*
166 silencing at different developmental time points. We were unable to silence the male-specific
167 splice variants (*NvDsxM*) of *NvDsx* specifically (Fig. S3B), therefore we targeted the common
168 region of *NvDsx* (*NvDsxU*). We observed that the developmental stage at which NvdsxU
169 dsRNA was injected greatly influenced a measurable decrease of *NvDsx* using qRT-PCR. We
170 found no significant decrease of *NvDsx* expression in 2nd instar *NvDsx* silenced males in
171 comparison to non-treated and *gfp* control when sampling after white pupal stage (Fig. S3*A*).
172 The strong increase of *NvDsx* expression from 2nd larval instar towards pupal stage (Fig. S3)

173 may be the root cause as the amount of siRNA present may be too limited to silence the
174 sudden increase of transcript amounts. However, this allowed us to transiently suppress
175 *NvDsx* during different developmental time windows. Injecting *NvDsxU* dsRNA in 4th instar
176 males led to a significant reduction of *NvDsx* in newly emerged adults when compared with
177 both non-treated (NT) (Tukey's HSD, P<.001) and *gfp* mock silenced males (Tukey's HSD,
178 P<.001), confirming successful *NvDsx* knockdown starting in the 4th instar male larvae with an
179 effect lasting into adulthood (Fig. S3*B*). *Gfp* mock silenced males also showed significant
180 reduction of *NvDsx* expression compared to NT (Tukey's HSD, P=0.021) suggesting that in
181 4th instar larvae there might be a non-target effects of *gfp* dsRNA as was shown before in
182 honey bee (32). Similar reduction in *NvDsx* silenced pupal stage males was observed when
183 sampling at adult stage compared to NT (Tukey's HSD, P=0.003) and *gfp* control (Tukey's
184 HSD, P=0.002) (Fig. S3*C*) which indicates that we also obtained a highly significant
185 knockdown of *NvDsx* from pupa stage onwards.

186 Non-treated and *gfp* dsRNA injected males showed unpigmented antennae and legs (Fig. 3*A*,
187 *B*, *C*), whereas females have pigmented antennae and legs (Fig. 3*D*). Depleting *NvDsx* from
188 the 2nd larval instar onwards increases the amount of pigmentation slightly (Fig. 3*F*), but
189 depleting *NvDsx* from male 4th instar larval stages onwards increases pigmentation in their
190 adult stage to the point that it resembled female-like pigmentation (Fig. 3*E*). No pigmentation
191 is observed in adult males when *NvDsx* is depleted from early white pupal stage onwards (Fig.
192 S4*B*).

193 Given the fact that we do not find changes in pigmentation intensity by *NvDsx* RNAi
194 experiments in 4th instar female larvae (Fig. S5*A* and *B*), and silencing *NvDsx* led to female-
195 like pigmentation in males, we conclude that female pigmentation is the default
196 developmental state and in males NvDsxM actively interferes with the melanin synthesis
197 pathway. As we find no true intersex phenotype, we hypothesize that NvDsxF plays no role in
198 enhancing the genes required for pigmentation in females. We observed a slight reduction in
199 antenna pigmentation of 4th instar *NvDsx* knockdown male larvae which is likely due to 1)
200 structural difference in the antennae with males having less plate organs on the subsegments
201 than females causing a different color reflection (33), and/or 2) incomplete knockdown of
202 *NvDsx.*

203 In *D. melanogaster,* expression of sex-specific abdominal pigmentation is regulated by
204 interaction of the HOX protein Abdominal-B (Abd-B) and Dsx. Combined input of Abd-B and
205 DsxF leads to the expression of *bric-a-brac* (*bab*) which suppresses the pigmentation in the
206 posterior abdomen segments while DsxM represses *bab* to maintain the posterior abdomen

207 pigmentation (8). In *Drosophila*, the deposition of the pigments in the cuticle starts from late
208 pupal to early adult stages (34), therefore, initiating the RNAi response from 4th instar larva in
209 *N. vitripennis* onwards creates enough time to deplete *NvDsx* mRNA and NvDsx protein
210 production to inhibit the expression of pigmentation genes.

211 ***NvDsx* silencing leads to increased forewing size of males**

212 The second sex-specific character that we assessed was forewing size and shape in
213 *N.vitripennis* adult males. Silencing *NvDsx* in both 2nd and 4th instar resulted in increased
214 forewing length, and width when compared to *gfp* mock silencing (Tukey's HSD, P<0.001)
215 and NT males (Tukey's HSD, P<0.001) (Fig. 4*B* and *C*). Length/width (L/W) ratio of *NvDsx*
216 knockdown treatments also showed severe reduction compared to *gfp* mock (Tukey's HSD,
217 P<0.001) and NT males (Tukey's HSD, P<0.001) (Fig. 4*A*) indicating that the wing got wider
218 and more female-like. However, the forewings of the *NvDsx* knockdown (*NvDsx-i*), mock *gfp*
219 (*gfp-i*) knockdown and non-treated males were still smaller and narrower than those of the
220 non-treated females (Length: Tukey's HSD, P<0.001; Width: Tukey's HSD, P<0.001; L/W
221 ratio: Tukey's HSD, P<0.001) (Fig. 4*A*, *B* and *C*). Interestingly, also here we found an effect of
222 timing as the forewing length and width increased significantly between 2nd and 4th instar
223 *NvDsx* treatments of which earlier stage *NvDsx* knockdown led to more severe changes
224 (Tukey's HSD, P<0.001), steering the L/W ratio towards NT female's dramatically (Tukey's
225 HSD, P<0.001). Between 2nd instar *gfp* and 4th instar *gfp* knockdown (Tukey's HSD,
226 P=0.062), 2nd instar *gfp* knockdown and NT (Tukey's HSD, P=0.070) and 4th instar *gfp*
227 knockdown and NT (Tukey's HSD, P=0.999) no significant difference were observed (Fig. 4*A*,
228 *B* and *C*). Depleting *NvDsx* from the white pupal stage onwards had no effect on forewing
229 size or shape (Fig. S4*F*).

230 Previous research showed that the non-coding region of *Dsx* in *N. giraulti*, the wing-size1
231 locus (*ws1*), is correlated with the development of long wings in males, and the *ws1* variant in
232 *N. vitripennis* is correlated with the severe reduced forewing size in males (35). Although
233 higher *NvDsxM1* expression levels was detected in individuals with the *N. vitripennis* ws1
234 variant (35), the mechanism of *NvDsx* regulation is unclear and the *NvDsxM2* and *-3* splice
235 variants were unknown at the time. Our research confirms that the regulation of the male
236 forewing size depends on high *NvDsxM* levels and illustrates the role of *NvDsxM* in
237 repressing wing growth. Changes in spatial and temporal expression of *unpaired-like* has
238 been shown to result in changes in wing width in *Nasonia* males caused by multiple
239 regulatory changes (36). NvDsxM regulation is likely responsible for differentially expressed
240 *upd-like*. In contrast to the observed complete female-specific pigmentation after *NvDsxM*

241 depletion in males, the depletion of *NvDsxM* from 2nd instar onwards is inadequate to restore
242 female forewing size. Wing size and shape development already takes place during
243 embryonal development and our chosen time window for RNAi is too late to induce a full
244 switch. We cannot rule out antagonistic effects of NvDsxM and NvDSXF on wing size
245 development in *Nasonia*, since in females *Aedes aegypti, Dsx* knockdown leads to smaller
246 wing development (37). However, we observed no wing size change after *NvDsx* knockdown
247 in females (Fig. S4*F*).

248 **Growth of male genitalia is controlled by *NvDsx***

249 Next, we depleted *NvDsx* at either 2nd or 4th instar larva stage to observe the role of *NvDsx* in
250 male genitalia development and growth after embryogenesis is completed. This is in contrast
251 to many studies being done using genome editing in which *Dsx* is knocked out from
252 embryogenesis onwards (10,12). *NvDsx* RNAi in both developmental stages reduced the
253 aedeagus length significantly when compared to *gfp* mock RNAi in both developmental
254 stages and NT males (Tukey's HSD, $P<0.001$) (Fig. 5A). Both developmental stages had the
255 same extent of reduction (Tukey's HSD, $P=0.998$). Aside from the shortened aedeagus, the
256 phallomere structure (genital phallic lobes) is also severely reduced in size in both 2nd and 4th
257 instar *NvDsx* depleted males (Fig. 5B-c and e) compared to *gfp* RNAi and NT males (Fig. 5B-
258 a, b and d) but the structure of the paramere including the outer parameres, cuspis and
259 digitus, is still intact (Fig. 5B). Compared to *gfp* RNAi males (Movie S1), the severe length
260 reduction of the aedeagus renders *NvDsx* RNAi males unable to copulate with a female
261 (Movie S2), showing that in this case size matters.

262 Dsx is shown to be involved in the differentiation of genitalia structures in male and female
263 insects in many cases by interactions with HOX genes during early embryogenesis (39).
264 However, whether Dsx is continuously required for genitalia development has not received
265 much attention. Previous studies using *Dsx* RNAi experiments in other species conducted at
266 late larval stage resulted in either deformed external genitalia or chimeras that contain the
267 structures of both sexes (24,29). Here, even though *NvDsx* RNAi was done at a distinctly
268 earlier stage (2nd instar larva) to other studied insect species, we could not observe any
269 abnormalities in genital organs other than size. This shows that contrary to other insects, in *N.*
270 *vitripennis* the differentiation of genital organs is completed before 2nd instar larval stage and
271 only growth is required during later development. It suggests that besides the sex-specific
272 tissue differentiation, *NvDsx* is also required for the direct sex-specific trait growth as it has
273 been shown in stag beetles *Cyclommatus metallifer* where it was demonstrated that *Dsx* can
274 manipulate the sensitivity of JH in a sex-specific way to regulate mandible growth in males

275 and females (14).

276 **Evolution of Dsx sex-specific OD2 domains and C-termini**

277 Aligning the OD2 domains of NvDsxM1, NvDsxM2 and NvDsxM3 (Fig. S6A) or NvDsxF (Fig.
278 S6B) with other DsxM or DsxF OD2 domains, respectively, shows that across insect orders
279 the male-specific OD2 domain is far less conserved than the female-specific OD2 domain.
280 Within insect orders, also a strong reduction of the sequence identity in male-specific OD2
281 domain alignment is seen. This observed rapid evolution of male-specific *dsx* regions is
282 supported by other research and is indicative of its fast evolution likely due to increased
283 diversity of secondary sexual traits in male insects (40). In females, the sex-specific region of
284 OD2 is relatively conserved across different insect orders. However, within Hymenoptera the
285 female-specific OD2 domain shows a lower similarity with only one out of eight conserved
286 amino acids being shared with all other tested species in the hymenopteran sequences, when
287 compared to other insect orders that have half of the conserved amino acids (Fig. S6B). In *D.*
288 *melanogaster* the C-terminus including the OD2 domain of DsxF binds the co-factor Intersex
289 (41). The differences in female-specific OD2 amino acid composition in Hymenoptera could
290 indicate that either no co-factors or different co-factors play a role in regulating the sex in this
291 order compared to the other insect orders. In addition, in Hymenoptera the female specific
292 OD2 domain was found to evolve much faster than the male-specific regions. This is contrary
293 to Diptera, Lepidoptera and Coleoptera and has been suggested to correlate with the
294 evolution of female-dominated eusociality and female-specific caste differentiation (40).
295 However, *Nasonia* is solitary as are many other hymenopteran species. In Hymenoptera,
296 females arise from fertilized eggs while male development initiates by default from haploid,
297 unfertilized eggs. We suggest that the rapid evolution of female-specific OD2 domain in
298 Hymenoptera could be linked to this difference. All in all, the identification of the two additional
299 male NvDsx isoforms opens the door to better comparative phylogenetic studies to better
300 understand the evolution of Dsx in insects.
301

302 **Outlook**

303 In this research we identified two sexually dimorphic traits and one male-specific trait that are
304 actively regulated during specific developmental windows by *Dsx* in *N. vitripennis.* Our results
305 suggest that male-specific lack of antennae and femur pigmentation is strictly regulated
306 during pupal development as silencing *NvDsx* from the larval stage onwards resulted in build-
307 up of pigmentation in the males, while silencing *NvDsx* from the pupal stage onwards did not

308 give any effect. In addition, our results suggest that sex-specific wing size and shape is
309 regulated by *NvDsx* during embryogenesis and early larval development as silencing *NvDsx*
310 from the 2nd larval instar onwards significantly increases wing size in males, while silencing
311 from the pupa onwards does not change wing size and shape. However, 2nd larval instar
312 *NvDsx* RNAi did not result in complete female-like wing size, suggesting that a big part of the
313 wing developmental window is during embryogenesis and possibly the 1st larval instar. We
314 additionally show that *NvDsx* regulates only male reproductive organ growth and not
315 morphology from 2nd larval instar onwards, suggesting that reproductive organ tissue
316 differentiation takes place before the 2nd instar which has not been reported before.
317 Visualizing *Dsx*-expressing cells in *D. melanogaster* has demonstrated before that *Dsx* gene
318 expression is under elaborate temporal and spatial control to regulate tissue-specific sexual
319 differentation (19). Here, we expand this knowledge using a non-drosophilid species by
320 showing that different morphological characteristics require their own specific timing and
321 action of Dsx protein and we speculate that this timing and action is also species-specific. Our
322 findings solidify the view that in insects, sexual development is not only a set and forget
323 mechanism that only operates during embryogenesis, but one that requires continuous input
324 from Dsx on a species-specific basis.

325 **Material and methods:**

326 **Insects rearing**

327 The *Nasonia vitripennis* lab strain AsymCx were reared on *Calliphora sp.* hosts *at* 16h/8h
328 light/dark and 25℃. AsymCx strain is in the lab for over 10 years and cured from *Wolbachia*
329 infection.

330 **5' and 3' RACE-PCR to identify additional *NvDsx* splice variants**

331 For identification of the 3' ends of *NvDsx* mRNA*,* total RNA of 3 adult male- and female
332 AsymCx wasps were extracted individually using TriZol (Invitrogen, Carlsbad, CA, USA) and
333 cleared from genomic DNA by using the DNA-*free* DNA removal kit according to
334 manufacturer's instructions (Invitrogen, Carlsbad, CA, USA). Total RNA was annealed with
335 the 3' adapter from the FirstChoice RLM-RACE kit (Ambion, Austin, TX, USA) during the
336 reverse-transcription using RevertAidTM H Minus First Strand cDNA Synthesis Kit
337 (Fermentas, Hanover, MD, USA) and stored at -80°C. The cDNA was subjected to series of
338 (semi-) nested PCRs using primers complementary to the adapter and gene-specific primers
339 targeting NvDSXU, and NvDsx_X7, NvDsx_X8, NvDsx_X9 and NvDSXMR1 at 94°C for 3

340 minutes, 35 cycles of 94°C for 30 seconds, 55-62°C for 30 seconds and 72°C for 2 minutes,
341 with a final extension of 10 minutes at 72°C. Primers were designed based on the initial
342 *NvDsx* gene structure (27) and sequences are listed in the Table S1.

343 For identification on the 5' end of *NvDsx*, total RNA of 3 female AsymCx wasps were
344 extracted using TriZol (Invitrogen, Carlsbad, CA, USA). After decapping, a 45-base RNA
345 adapter has been ligated to the RNA population using the FirstChoice RLM-RACE kit (Ambion,
346 Austin, TX, USA) and reverse transcribed using the RevertAidTM H Minus First Strand cDNA
347 Synthesis Kit (Fermentas, Hanover, MD, USA). The cDNA was subjected to series of (semi-)
348 nested PCRs using primers complementary to the adapter and gene-specific primers
349 targeting NvDSXU at 94°C for 3 minutes, 35 cycles of 94°C for 30 seconds, 55-60°C for 30
350 seconds and 72°C for 2 minutes, with a final extension of 10 minutes at 72°C. Primers were
351 designed based on the initial *NvDsx* gene structure (27) and sequences are listed in the Table
352 S1.

353 5' and 3' RACE-PCR fragments were run and visualized on ethidium bromide-containing
354 1.5% agarose gel with 1×TAE buffer. All RACE-PCR products were purified using GeneJET
355 Gel Purification Kit (Fermentas, Hanover, MD, USA) and ligated into pGEM-T vector
356 (Promega, Madison, WI, USA) and transformed into competent JM-109 *Escherichia coli* cells
357 (Promega, Madison, WI, USA). Colony-PCRs were conducted by using primers
358 recommended by the kit at 94°C for 3 minutes, 40 cycles of 94°C for 30 seconds, 55°C for 30
359 seconds and 72°C for 2 minutes, with a final extension of 7 minutes at 72°C. All isoforms
360 were sequenced on an ABI 3730XL capillary sequencer (Applied Biosystems) and reads were
361 visualized and aligned in MEGA4 (42). Exon-intron structure of the genes was constructed by
362 aligning the mRNA sequences to *N. vitripennis* genome and visualizing with Geneious Prime
363 2019.1.3 and CLC Workbench 6.

364 **RT-PCR to confirm usage of alternative 1' exon**

365 Total RNA was extracted from four female samples and three male samples containing three
366 adults each using NucleoSpin XS (Brand) with final elution done in 15 µl nuclease-free water.
367 Eleven µl of eluted total RNA was converted to cDNA using RevertAidTM H Minus First
368 Strand cDNA Synthesis Kit (Fermentas, Hanover, MD, USA) with random hexamers
369 according to manufacturer's protocol and stored at -80°C. One female sample was not
370 converted to cDNA but used as gDNA contamination control in RT-PCR. For the RT-PCR
371 reactions with the primersets NvEF-1a (Table S1) and Nv_DsxU_F6 or Nv_DsxU_F7 with
372 Nv_Dsx_qPCR_R, GoTaq® G2 Flexi DNA Polymerase (Promega) was used to prepare the
373 mastermix following manufacturer's instruction and amplified with a standard PCR profile: 3

374 min at 95°C, 35 amplification cycles of 30s at 95°C, 30s at 55°C, 30s at 72°C and a final
375 extension of 7 min at 72 °C in a thermal cycler (T100TM Thermal Cycler, Bio-Rad). Five µl of
376 PCR product was visualized on a non-denaturing 1% agarose gel with a 100bp ladder. PCR
377 fragments were Sanger sequenced at Eurofins Scientific to confirm correct amplification.

378 **Alignment and phylogenetic analysis of Dsx OD2 domain across insect orders**

379 Dsx isoforms from 22 species across insect taxa were downloaded from NCBI protein
380 database with accession number attached in the end of each sequence name (Fig. S6A and
381 S6B). OD2 common domain and sex-specific region of OD2 domain selection is based on An
382 et al. 1996 (2). Both the male and female Dsx OD2 domain sequences were separately
383 aligned using Guidance2 Online Server with Guidance2 method, settings are MAFFT
384 algorithm, maxiteration of 10, 100 alternative guide-trees. Geneious 2019.1 (created by
385 Biomatters. Available from https://www.geneious.com) was used to shade the amino acids
386 with Blosum62 score matrix applied to display the similarity between each sequence
387 (threshold at 3).

388 **RNAi of *NvTraF* and *NvDsx* gene**

389 For the *Nvtra* RNAi knockdowns, MEGAscript RNAi Kit (Thermo Fisher) was used to generate
390 dsRNA to target exon 5-8 of *Nvtra* mRNA in 4th instar larva stage of females which resulted in
391 a male splice form of *NvDsx* as shown in Verhulst *et al.* (28). To conduct functional analysis of
392 *NvDsx*, MEGAscript RNAi Kit (Thermo Fisher) was used to generate dsRNA based on *NvDsx*
393 common region (exon 2-5) present in both male and female splice-variants or the specific
394 region (exon 7-9) only presents in two longer male splice-variants. *Gfp* dsRNA was generated
395 from the vector pOPINEneo-3C-GFP and was a gift from Ray Owens (Addgene plasmid #
396 53534; http://n2t.net/addgene: 53534; RRID: Addgene_53534). This *gfp* dsRNA was used as
397 control in all experiments as it has no target in *Nasonia*. Primers designed using Geneious
398 10.0.9 to construct the dsRNA T7 template are listed in the Table S1. For male-specific
399 *NvDsx* RNAi, offspring of AsymCX strain was collected at 2nd and 4th larval instars and white
400 pupa stages which are described in Table S2. All dsRNAs were diluted with RNase-free
401 elution buffer (MEGAscript RNAi Kit (Thermo Fisher)) to 4000 ng/ul (NanoDrop™ 2000
402 Spectrophotometer, ThermoFisher) before proceeding to microinjection.

403 Microinjection of different developmental stages of wasps was carried out with IM300
404 Microinjecctor (Narishige) and FemtoJet® 4i (eppendorf) which followed the protocols
405 described by Werren *et al*. (43) and Lynch & Desplan (44) with minor changes. Red colour
406 food dye was pre-mixed with the dsRNAs in a ratio of 1:9. Experiments were performed using

407 AsymCx strain at different developmental stages for different purposes (Table S3).

408 2nd and 4th instar larvae were collected from parasitoid hosts and placed on a 1X PBS agar
409 plate before injection. Early pupal stage samples were fixed on the glass slides with double-
410 sided tape. After injection, 2nd instar larvae were transferred back to host (6-8 per host) and
411 sealed with the host shell. Afterward, sealed hosts were kept in 8 tube-PCR strips with open
412 lid. Subsequently, all injected samples either in 8 tube-PCR strip or on slides were placed on
413 1X PBS plates to prevent dehydration and incubated at standard rearing conditions until adult
414 emergence.

415 ***NvDsx* splicing and expression throughout development**

416 Male and female wasps were separated at black pupal stage by the sex-specific traits such as
417 forewing size and presence/absence of the ovipositor. To generate female offspring, one
418 selected male and one selected female pupa were collected in a single glass vial clogged with
419 cotton plug until eclosion and kept for one more day to make sure they had mated. After
420 fertilization, two hosts per day for the first two days were provided to mated females to initiate
421 oviposition. Afterwards, one-hour host presentations were repeated twice in a row per day.
422 Since mated *N. vitripennis* tend to lay extremely female-biased eggs, offspring from mated
423 females was considered female (45). Male offspring was collected by using virgin females
424 with the same setup. To facilitate early stage (eggs) sample collection, egg-laying chamber
425 (1.5ml Eppendorf tube with cut-off tip presenting the head of host pupa plugged in 1000 µL
426 filter pipet tip) was made to allow the female only access to the head portion of the fly host.

427 To confirm that male-specific splice variants were not under the regulation of NvTraF but
428 spliced in default mode independently of NvTraF, female samples were collected from 3h, 1d,
429 2d, 3d, 4d, 5d and 6d after Nv*traF* knockdown. To study the expression pattern of *NvDsx* sex-
430 specific splice variants throughout whole developmental stages, samples were collected at
431 specific time points listed in Table S2. More than 50 embryo eggs were collected at 36h and
432 five to ten larvae, pupae or adults were collected at 2.5d and onwards. Collected samples
433 were subsequently frozen in liquid nitrogen and stored in -80°C. *NvDsx* sex-specific primers
434 were designed using Geneious 10.0.9. Both RP49 and NvEF-1a were assessed for their
435 expression stability in this semi-quantitative RT-PCR setup, and *NvEF-1a* was finally chosen
436 as the reference gene. Primer sequences are listed in the Table S1.

437 Frozen samples were homogenized by pestles which were designed for 1.5 ml
438 microcentrifuge tubes (Biosphere SafeSeal Tube 1.5ml). Total RNA was extracted using ZR
439 Tissue & Insect RNA MicroPrep™(Zymo) following manufacturer's instructions. On column

440 DNase treatment step was added to all samples. Total RNA of each samples was eluted in 16
441 µl of DNase/RNase free water. After verifying the purity and concentration by NanoDrop™
442 2000 Spectrophotometer (ThermoFisher), 1µg of each template was synthesized into cDNA
443 with standard reaction mix (SensiFAST™ cDNA Synthesis Kit, Bioline) in a thermal cycler
444 (Bio-Rad T100TM Thermal Cycler, Bio-Rad) with 5 min priming at 25°C, 30 min reverse
445 transcription at 46°C and 5 min reverse transcriptase inactivation at 85°C.

446 For all RT-PCR reactions, GoTaq® G2 Flexi DNA Polymerase (Promega) was used to
447 prepare the mastermix following manufacture's instruction and amplified with a standard PCR
448 profile: 3min at 95°C, 34 (male-specific splicing verification) / 29 (expression pattern of *NvDsx*)
449 amplification cycles of 30s at 95°C, 30s at 55°C, 50s at 72°C and a final extension of 5 min at
450 72 °C in a thermal cycler (T100TM Thermal Cycler, Bio-Rad). In order to standardize the
451 expression pattern of *NvDsx*, the number of PCR cycles needed was determined by
452 comparison of the brightness of the bands in gels of different PCR reactions with cycles
453 ranging from 25 to 34 cycles to achieve non-oversaturated brightness. In the end 29 cycles
454 were used for both reference genes and target genes.

455 **Silencing efficiency of *NvDsx***

456 qPCR was conducted to verify the silencing efficiency of *Dsx* knockdown. After *dsRNA*
457 injection, samples were collected at either adult stages (injected at 4th instar larva and white
458 pupa stages) or white pupa stage (injected at 2nd instar larva stage). Four to five pupae or
459 adults were pooled to produce one biological replicate and six replicates per treatment were
460 prepared. All testing samples were used in qPCR according to SensiFAST^{TM} SYBR® No-
461 ROX Kit manual (Bioline). *NvDsx* qPCR primers were designed on the common region (exon
462 3-5) of male and female splice variants (Table S1). *NvEF-1a* was used as reference genes.
463 qPCR was carried out using the CFX96TM Real-Time System (Bio-Rad) with Bio-Rad CFX
464 Manager 3.1 Software (Bio-Rad). The standard qPCR profiles consist of 95°C for 3min, 45
465 amplification cycles of 15s at 95,15s of 55°C, 30s of 72°C with a final standard dissociation
466 curve step to check for non-specific amplification.

467 **Measurements of male forewing size, external reproduction organs**

468 Forewing size was measured by wing length and width based on the standard methods
469 described by Loehlin *et al.* (46). Tibia length of the hind leg was used to standardize the body
470 size differences among individuals (47). Forewings and external reproduction organ of adult
471 males were dissected on clean slides with a drop of 1%PBS buffer using dissection tweezers
472 and subsequently mounted in a drop of ethanol on slides which was allowed to evaporate.

External reproduction apparatuses were identified based on the description in Liu et al (48) and E. Snodgrass (38). Photos were taken and measured by Dino-Lite Edge 5MP digital microscope using DinoCapture 2.0 software.

Data analysis

qPCR data was imported to LinRegPCR software (LinRegPCR, 2017.1.0.0, HFRC, Amsterdam, The Netherlands) (49). After baseline correction, the initial number of templates (N0) were calculated based on the average PCR efficiency of each amplicon. Relative expression levels of *NvDsx* in each sample was obtained by dividing the N0 value of *NvDsx* by N0 value of *EF-1a*. Statistical analysis of qPCR and measurement data was performed in R using One-way ANOVA and Tukey's Honest Significant Difference (HSD) for post hoc test.

Acknowledgment

We thank Hans Smid for assisting with the phenotype recording; Rutger Diepeveen for his contribution to the *NvDsx* RNAi work; Joan Diaz Calafat, Age Muller, Simon Pleiter and Romy Gielings for their contribution to the *NvtraF* RNAi work; Min Xu for supporting the sample preparation, collection and measuring; and Weizhao Sun for recording the mating behaviour of RNAi treated males. We additionally thank all the tested *N. vitripennis* for their great sacrifice to science. This work is part of the Dutch Research Council (NWO) research programme Innovational Research Incentives Scheme Veni with project number 863.13.014 granted to ECV.

493 **Reference**

494 1. O. Barmina and A. Kopp, Sex-specific expression of a HOX gene associated with rapid
495 morphological evolution. *Dev. Biol.* **311**, 277–286 (2007).

496 2. W. An, S. Cho, H. Ishii and P. C. Wensink, Sex-specific and non-sex-specific
497 oligomerization domains in both of the *doublesex* transcription factors from *Drosophila*
498 *melanogaster*. *Mol. Cell. Biol.* **16**, 3106–11 (1996).

499 3. J. N. Shukla and S. R. Palli, Doublesex target genes in the red flour beetle, *Tribolium*
500 *castaneum*. *Sci. Rep.* **2**, 948 (2012).

501 4. F. Ohbayashi *et al*., A homologue of the *Drosophila doublesex* gene is transcribed into sex-
502 specific mRNA isoforms in the silkworm, *Bombyx mori*, *Comp. Biochem. Physiol. - B Biochem.*
503 *Mol. Biol.* **128**, 145-158 (2001).

504 5. K. C. Burtis and B. S. Baker, *Drosophila doublesex* gene controls somatic sexual
505 differentiation by producing alternatively spliced mRNAs encoding related sex-specific
506 polypeptides. *Cell.* **56**, 997–1010 (1989).

507 6. D. C. Price, A. Egizi and D. M. Fonseca, The ubiquity and ancestry of insect *doublesex*. *Sci.*
508 *Rep.* **5**, 13068 (2015).

509 7. E. C. Verhulst and L. van de Zande, Double nexus-Doublesex is the connecting element in
510 sex determination. *Brief. Funct. Genomics* **14**, 396–406 (2015).

511 8. T. M. Williams *et al*., The Regulation and Evolution of a Genetic Switch Controlling Sexually
512 Dimorphic Traits in *Drosophila*. *Cell* **134**, 610–623 (2008).

513 9. A. Kopp, *Drosophila* sex combs as a model of evolutionary innovations. *Evol. Dev.* **13**,
514 504–22 (2011).

515 10. X. Chen *et al*., Disruption of sex-specific *doublesex* exons results in male- and female-
516 specific defects in the black cutworm, *Agrotis ipsilon*. *Pest Manag. Sci.* **75**, 1697-1706 (2019).

517 11. M. G. Suzuki *et al*., Role of the male BmDSX protein in the sexual differentiation of
518 *Bombyx mori*. *Evol. Dev.* **7**, 58–68 (2005).

519 12. J. Xu *et al*., Sexually dimorphic traits in the silkworm, *Bombyx mori*, are regulated by
520 *doublesex*. *Insect Biochem. Mol. Biol.* **80**, 42–51 (2017).

521 13. K. Kunte *et al*., *doublesex* is a mimicry supergene. *Nature* **507**, 229–232 (2014).

522 14. H. Gotoh *et al*., Developmental link between sex and nutrition; *doublesex* regulates sex-
523 specific mandible growth via juvenile hormone signalling in stag beetles. *PLoS Genet.* **10**,
524 e1004098 (2014).

525 15. Y. Ito *et al*., The role of *doublesex* in the evolution of exaggerated horns in the Japanese
526 rhinoceros beetle. *EMBO Rep.* **14**, 561–567 (2013).

527 16. C. C. Ledón-Rettig, E. E. Zattara and A. P. Moczek, Asymmetric interactions between
528 *doublesex* and tissue- and sex-specific target genes mediate sexual dimorphism in beetles.
529 *Nat. Commun.* **8**, 14593 (2017).

530 17. C. C. Robinett, A. G. Vaughan, J.-M. Knapp and B. S. Baker, Sex and the single cell. II.
531 There is a time and place for sex. *PLoS Biol.* **8**, e1000365 (2010).

532 18. J. L. Morrow, M. Riegler, M. Frommer and D. C. A. Shearman, Expression patterns of
533 sex-determination genes in single male and female embryos of two *Bactrocera* fruit fly
534 species during early development. *Insect Mol. Biol.* **23**, 754–767 (2014).

535 19. A. Klein *et al*., Evolution of social insect polyphenism facilitated by the sex differentiation
536 cascade, *PLOS Genet.* **12**, e1005952 (2016).

537 20. M. Nipitwattanaphon *et al*., Effects of ploidy and sex-locus genotype on gene expression
538 patterns in the fire ant *Solenopsis invicta*. *Proc. R. Soc. B Biol. Sci.* **281**, 20141776–20141776
539 (2014).

540 21. S. Cho, Z. Y. Huang and J. Zhang, Sex-specific splicing of the honeybee *doublesex* gene
541 reveals 300 million years of evolution at the bottom of the insect sex-determination pathway.
542 *Genetics* **177**, 1733–41 (2007).

543 22. A. Ugajin *et al*., Expression profile of the sex determination gene *doublesex* in a
544 gynandromorph of bumblebee, *Bombus ignites*. *Sci. Nat.* **103**, 17 (2016).

545 23. M. O. Miyakawa, K. Tsuchida and H. Miyakawa, The *doublesex* gene integrates multi-
546 locus complementary sex determination signals in the Japanese ant, *Vollenhovia emeryi*.
547 *Insect Biochem. Mol. Biol.* **94**, 42–49 (2018).

548 24. S. Mine *et al*., Identification and functional characterization of the sex-determining gene
549 *doublesex* in the sawfly, *Athalia rosae* (Hymenoptera: Tenthredinidae). *Appl. Entomol. Zool.*
550 **52**, 497–509 (2017).

551 25. R. Raychoudhury *et al*., Behavioral and genetic characteristics of a new species of
552 *Nasonia*, *Heredity.* **104**, 278–288 (2010).

553 26. D. C. Darling and J. H. Werren, Biosystematics of *Nasonia* (Hymenoptera: Pteromalidae):
554 Two new species reared from birds' nests in north America. *Ann. Entomol. Soc. Am.* **83**, 352–
555 370 (1990).

556 27. D. C. S. G. Oliveira *et al*., Identification and characterization of the *doublesex* gene of
557 *Nasonia*. *Insect Mol. Biol.* **18**, 315–324 (2009).

558 28. E. C. Verhulst, L. W. Beukeboom and L. van de Zande, Maternal control of haplodiploid
559 sex determination in the wasp *Nasonia*. *Science.* **328**, 620–623 (2010).

560 29. J.-C. Zhuo *et al*., Identification and functional analysis of the *doublesex* gene in the sexual
561 development of a hemimetabolous insect, the brown planthopper. *Insect Biochem. Mol. Biol.*
562 **102**, 31–42 (2018).

563 30. B. S. Baker and M. F. Wolfner, A molecular analysis of *doublesex*, a bifunctional gene that
564 controls both male and female sexual differentiation in *Drosophila melanogaster*. *Genes Dev.*
565 **2**, 477–489 (1988).

566 31. J. N. Shukla and J. Nagaraju, Two female-specific DSX proteins are encoded by the sex-
567 specific transcripts of *dsx*, and are required for female sexual differentiation in two wild
568 silkmoth species, *Antheraea assama* and *Antheraea mylitta* (Lepidoptera, Saturniidae). *Insect*
569 *Biochem. Mol. Biol.* **40**, 672–682 (2010).

570 32. F. Nunes *et al*., Non-target effects of green fluorescent protein (GFP)-derived double-
571 stranded RNA (dsRNA-GFP) used in honey bee RNA interference (RNAi) assays, *Insects* **4**,
572 90–103 (2013).

573 33. E. H. Slifer, Sense organs on the antenna of a parasitic wasp, *Nasonia vitripennis*
574 (Hymenoptera, Pteromalidae). *Biol. Bull.* **136**, 253–263 (1969).

575 34. J. H. Massey and P. J. Wittkopp, The genetic basis of pigmentation differences within and
576 between *Drosophila* species. *Curr. Top. Dev. Biol.* **119**, 27-61.

577 35. D. W. Loehlin *et al*., Non-coding changes cause sex-specific wing size differences
578 between closely related species of *Nasonia*, *PLoS Genet.* **6**, e1000821 (2010).

579 36. D. W. Loehlin and J. H. Werren, Evolution of shape by multiple regulatory changes to a
580 growth gene. *Science* **335**, 943–7 (2012).

581 37. K. Mysore et al., siRNA-mediated silencing of *doublesex* during female development of
582 the dengue vector mosquito *Aedes aegypti*. *PLoS Negl. Trop. Dis.* **9**, e0004213 (2015).

583 38. R. E. Snodgrass, A revised interpretation of the external reproductive organs of male
584 insects. *Smithson. Misc. Collect.* **136**, 1–60 (1957).

585 39. A. E. Christiansen, E. L. Keisman, S. M. Ahmad and B. S. Baker, Sex comes in from the
586 cold: the integration of sex and pattern. *Trends Genet.* **18**, 510–516 (2002).

587 40. S. Baral, G. Arumugam, R. Deshmukh and K. Kunte, Genetic architecture and sex-
588 specific selection govern modular, male-biased evolution of *doublesex*. *Sci. Adv.* **5**, eaau3753
589 (2019).

590 41. Y. Yang, W. Zhang, J. R. Bayrer and M. A. Weiss, *Doublesex* and the regulation of sexual
591 dimorphism in *Drosophila melanogaster*. *J. Biol. Chem.* **283**, 7280–7292 (2008).

592 42. K. Tamura, J. Dudley, M. Nei and S. Kumar, MEGA4: Molecular evolutionary genetics
593 analysis (MEGA) software version 4.0. *Mol. Biol. Evol.* **24**, 1596–1599 (2007).

594 43. J. H. Werren, D. W. Loehlin and J. D. Giebel, Larval RNAi in *Nasonia* (parasitoid wasp).
595 *Cold Spring Harb. Protoc.* DOI:10.1101/pdb.prot5311 (2009).

596 44. J. A. Lynch and C. Desplan, A method for parental RNA interference in the wasp *Nasonia*
597 *vitripennis*. *Nat. Protoc.* **1**, 486–494 (2006).

598 45. W. D. Hamilton, Extraordinary sex ratios. *Science.* **156**, 477–488 (1967).

599 46. D. W. Loehlin, L. S. Enders and J. H. Werren, Evolution of sex-specific wing shape at the
600 widerwing locus in four species of *Nasonia*. *Heredity.* **104**, 260–269 (2010).

601 47. H. C. J. Godfray, Parasitoids: behavioral and evolutionary ecology. *Parasitoids Behav.*
602 *Evol. Ecol.* (1994).

603 48. N.-Y. Liu *et al*., Morphology and ultrastructure of the male reproductive system of the
604 jewel wasp, *Nasonia vitripennis* (Walker) (Hymenoptera: Pteromalidae). *J. Asia. Pac. Entomol.*
605 **20**, 577–582 (2017).

606 49. C. Ramakers, J. M. Ruijter, R. H. L. Deprez and A. F. Moorman, Assumption-free analysis
607 of quantitative real-time polymerase chain reaction (PCR) data. *Neurosci. Lett.* **339**, 62–66
608 (2003).

609

610 **Figures**

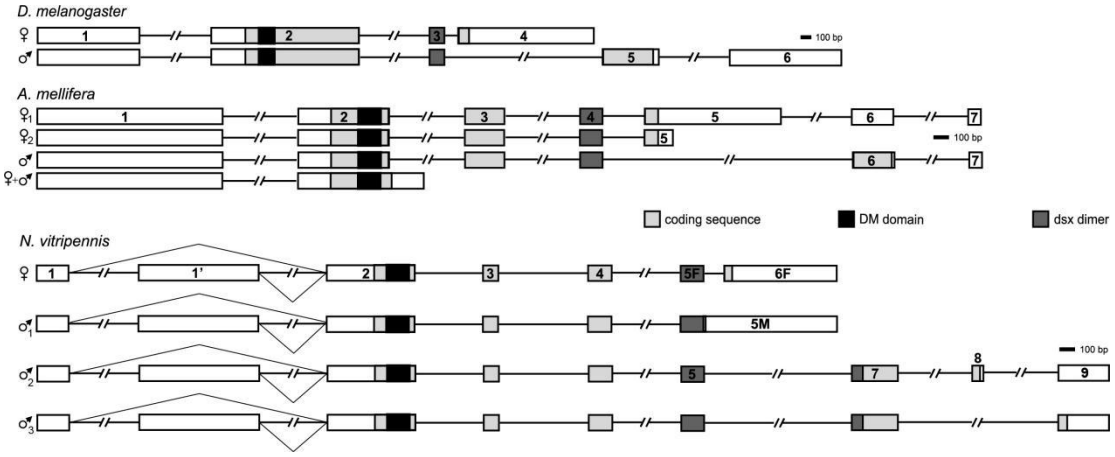

611

612 Figure 1. Comparison of insect *Doublesex* (*Dsx*) gene models. The eight *N. vitripennis* male
613 and female *Dsx* splice variants are compared to *Dsx* splice variants of *D. melanogaster* and *A.*
614 *mellifera*. Figure was modified from Oliveira *et al.* (27) to include the alternative 1st exon (1')
615 and the additional *NvDsx* male splice variants. Male and female specific splice forms are
616 indicated by ♂ and ♀. Exon numbers are noted on each exon. Light grey, black and dark grey
617 blocks indicate coding region, DM domain and OD2 dsx dimer region respectively. Scales are
618 provided behind each species splice structures.

619

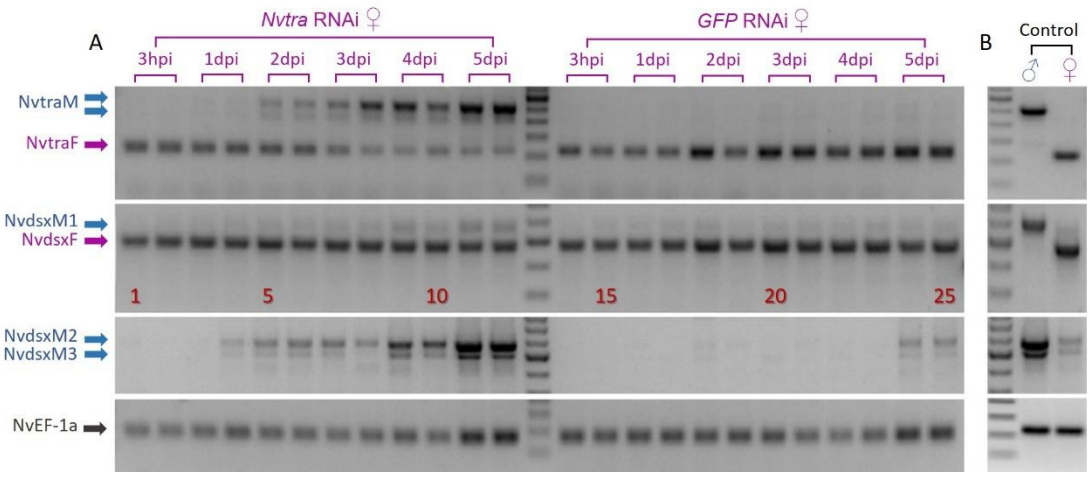

Figure 2. Confirmation of sex-specific *Dsx* splicing after *Nvtra* knockdown in *N.vitripennis.* (A) Sex-specific splice variants of *Nvtra* and *NvDsx* in *N. vitripennis* females that are injected in the 4th instar larval stage with *Nvtra* dsRNA or *gfp* dsRNA. (B) male and female non-treated (NT) control samples for each primer sets. Arrows indicate male (in blue) and female (in pink) splice forms of the different genes. Lanes 1-12: Female *Nvtra* knockdown samples from 3-hour post injection (hpi) to 5-day post injection (dpi). Lane 13: 100bp ladder (Thermo). Lanes 14-25: Female *gfp* knockdown samples from 3dpi to 5dpi. For each stage two samples are used. *EF-1a* is used as expression and loading control.

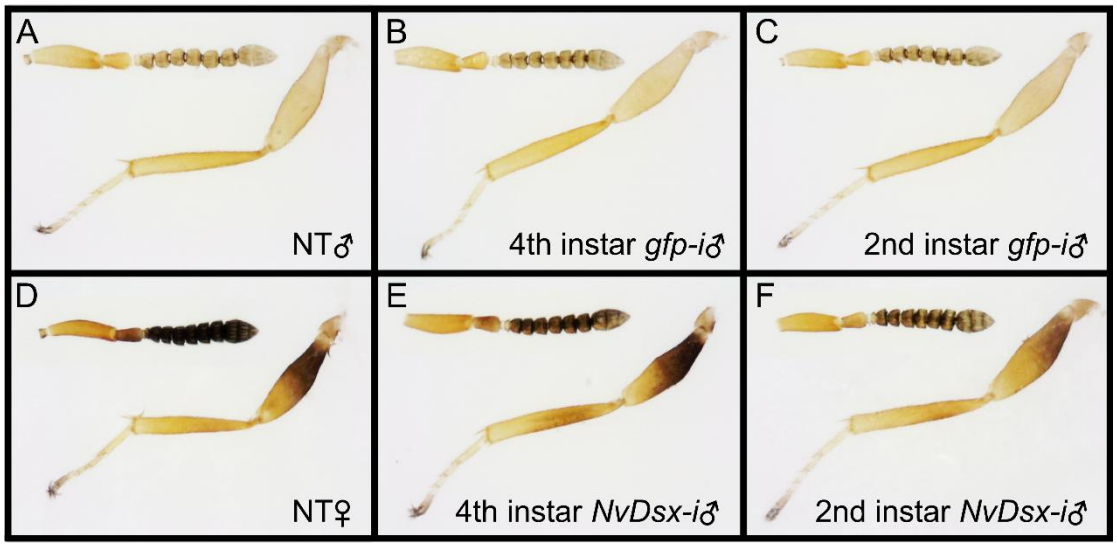

Figure 3. Pigmentations of antennae and hind legs of adult wasps after RNAi treatment in different developmental stages. (A) NT male (B) 4th instar *gfp* RNAi (*gfp-i*) male (C) 2nd instar *gfp* RNAi (*gfp-i*) male (D) NT female (E) 4th instar *NvDsx* RNAi (*NvDsx-i*) male and (F) 2nd instar *NvDsx* RNAi (*NvDsx-i*) male. Light source and exposure time are equal in all pictures.

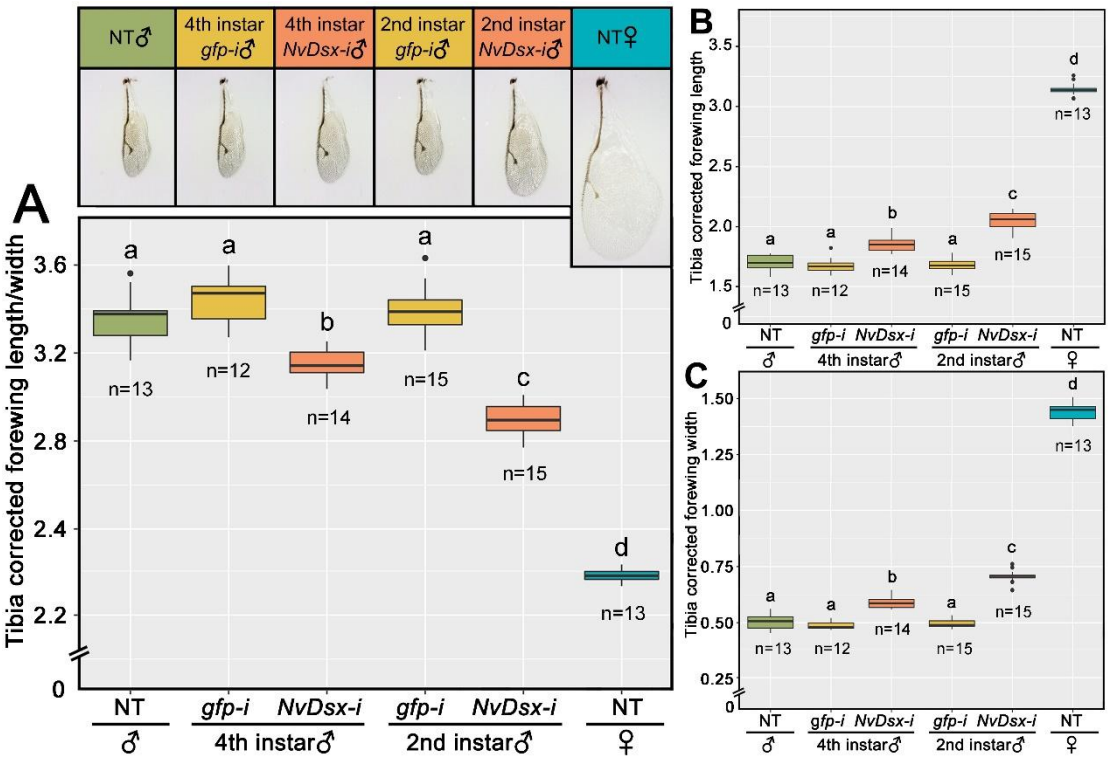

Figure 4. Comparision of forewing size of adult males after *NvDsx* (*NvDsx-i*) or mock *gfp* (*gfp-i*) dsRNA treatment in the 2nd or 4th instar larval stage and NT control. Y-axis represent (A) forwing length/width ratio corrected with tibia length; (B) length corrected with tibia length; (C) width corrected with tibia length. X-axis shows 6 different groups: males treated with *NvDsx* (*NvDsx-i*) and *gfp* (*gfp-i*) dsRNA in the 2nd and 4th instar larval stage, NT males and NT females. Different colors were assigned for different treatments. Boxplots were generated in R and displayed with minimum, first quartile (Q1), median, third quartile (Q3), and maximum. Dots outside the boxplots represent outliers from the treatments. Replicates were provided in the figures of each treatment. One-way ANOVA and post-hoc Tukey's HSD were used for data analysis. Letters in the figures denote statistical significance (P<0.05) among treatments.

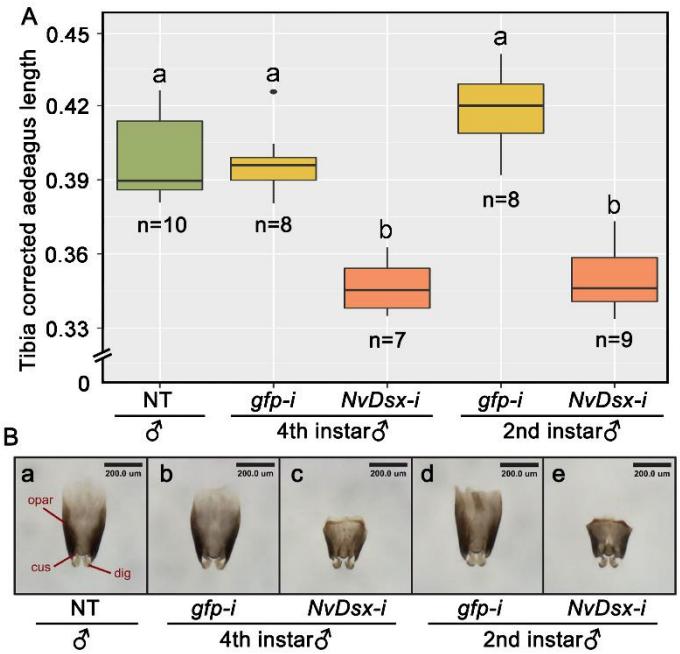

Figure 5. Comparison of genitalia length of adult males after *NvDsx* (*NvDsx-i*) or mock *gfp* (*gfp-i*) dsRNA treatment in the 2nd or 4th instar larval stage and NT control. A) Y-axis represents genitalia length corrected with tibia length. X axis shows 5 experiment groups: males treated with *NvDsx* (*NvDsx-i*) and *gfp* (*gfp-i*) dsRNA in the 2nd and 4th instar larval stage and NT control. Different colours were assigned for different treatments. Boxplots were generated in R and displayed with minimum, first quartile (Q1), median, third quartile (Q3), and maximum. Dots outside the boxplot represent outliers from each treatment. Replicates were provided in the figures of each treatment. One-way ANOVA and post hoc Tukey's HSD were used for data analysis. Letters in the figures denote statistical significance ($P<0.05$) among treatments. B) Comparison of paramere length (without aedeagus) of adult males after *NvDsx* or mock *gfp* dsRNA treatment in the 2nd or 4th instar larval stage and NT control. (a) paramere length (without aedeagus) in NT males, (b and d) after treatment with *NvDsx* (*NvDsx-i*) dsRNA in 4th and 2nd instar male larvae, (c and e) after treament with *gfp* (*gfp-i*) dsRNA in 4th and 2nd instar larvae. Different treatments are indicated below the figure. Scales are provided on top of each photos. Each part of paramere is described in *E. Snodgrass (1957)* (38) and indicated with the following abbreviations: outer parameres (opar), cuspis (cus) and digitus (dig).